FOIL-LEVEL FABRICATION OF INKJET-PRINTED PYROMEMS BALLOON ACTUATORS

D.A. de Koninck, F. Molina Lopez, D. Briand, and N.F. de Rooij
Ecole Polytechnique Fédérale de Lausanne (EPFL), STI IMT SAMLAB, Neuchâtel, SWITZERLAND

ABSTRACT

The fabrication, modeling and testing of a pyroMEMS balloon actuators are presented herein. A foil-level fabrication method was developed, integrating nickel-plated, inkjet-printed igniters capable of generating >200 °C for ~1 s—sufficient for fuel combustion—and a low-temperature (120 °C) lamination technique using thick photodefinable epoxy sheets. Two different fuel mixtures and three different chamber volumes were tested. Balloon actuators (5 mm dia.) were successfully inflated, reaching over 5 mm in height. Maximum balloon heights were in good agreement with the semi-analytical model developed (28-35 % over prediction).

INTRODUCTION

This communication presents a foil-level fabrication, modeling and testing of pyroMEMS balloon actuators. The fabrication method leverages low-cost polymer substrates, additive processing—such as inkjet printing and electroplating—and low-temperature lamination. Specifically, this paper presents: (1) nickel-plated, inkjet-printed Joule-effect igniters capable of sustaining >200 °C for short times (on the order of 1 second), and; (2) a low-temperature (120 °C), foil-level lamination method using thick, photodefinable epoxy dry films.

Pyrotechnical microsystem (PyroMEMS) balloon actuators consist of a solid propellant charge deposited within a small micro-fabricated cavity covered by a flexible membrane. Combustion of the propellant generates high-pressure gas, which inflates the membrane to do work. Potential applications include disposable fluid actuators for drug delivery [1] and microfluidic systems [2]. This work will demonstrate fuel ignition and combustion as well as balloon inflation dynamics using a high-speed framing camera. A semi-analytical model of the pyroMEMS balloon actuation was also developed.

A proof of concept pyroMEMS balloon actuator was previously presented at MEMS 2008 [3] out of silicon and glass substrates using standard cleanroom fabrication techniques. Rodríguez et al. [2] have also demonstrated similar silicon-based devices. However, due to their single-use nature, pyroMEMS are particularly suited to low-cost, large-scale fabrication techniques—such as on plastic foils.

FABRICATION

The device consisted of three different layers: (1) a plastic foil with a fuel-covered Joule-effect igniter, (2) an epoxy chamber, and (3) a PDMS membrane. Each layer was processed at the foil-level then diced/cut into 2x2 matrices for lamination. In total, 56 balloon actuators were fabricated.

Propellant

The propellant paste used consisted of a mixture of potassium dinitrobenzofuroxanate (K-DNBF), a water-based binder (Adhesin® by Henkel) and solvent (water)—which evaporated after the deposition yielding a solid propellant drop on the igniter. K-DNBF was chosen due to its relatively low ignition temperature and large volume of gas generated. It is a so-called "green propellant"—i.e., it does not contain heavy metals—whose primary combustion product is CO_2. Two different binder mass fractions were tested: 10 and 20 %. The ignition temperature of pure K-DNBF—as measured by differential scanning calorimetry—is 206±5 °C and decreases to 203±5 °C for a binder mass fraction of 20 %. The fuel paste was manually drop coated using a dispensing gun (Fishman LDS 9000). The 10 % binder fuel drops weighed 320 ± 70 µg, while the 20 % binder drops weighed 420 ± 100 µg. The drop measured 2.0 ± 0.2 mm in diameter.

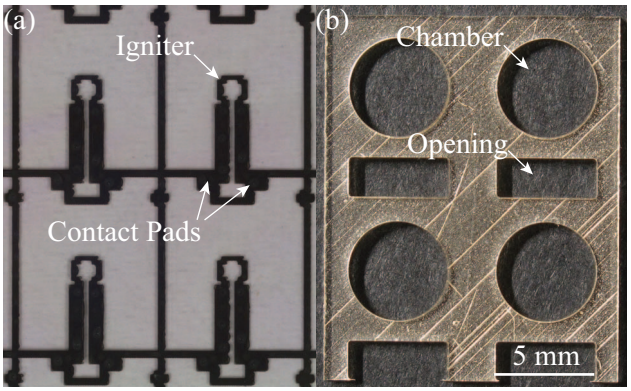

Figure 1: Photographs of 2x2 matrices of: (a) inkjet-printed igniters and (b) epoxy chambers.

Inkjet-printed Igniters

The igniters consisted of an annular igniter, two wide interconnects—to minimize any stray heating—and two large contact pads (Figure 1a). The annular shape helps prevent fuel ejection [4]. The heated area measured roughly 1.5 mm x 1.5 mm with a nominal line width of 200 µm. The igniters were all shorted electrically for nickel electroplating. Prior to lamination, those connections were removed manually with a scalpel.

The high-temperature igniters were fabricated using a two-step process: first, a 180 nm seed layer of silver nanoparticles was inkjet-printed onto the plastic foil, followed by 500-nm nickel electroplating of the igniters. The nickel-plating was needed for the igniters to sustain the current densities required for fuel ignition (see below).

The devices were fabricated on a 125-µm thick polyethylene terephthalate (PET) foil (Dupont Melinex ST506). PET was chosen due to its low cost, commercial availability and its suitability for inkjet printing. Prior to

printing, the substrates were dehydrated for a minimum of 1 hour in an oven at 120 °C and then treated with microwave oxygen plasma (PVA TePla PS210) for 4 minutes (400 sccm, 400 W).

Inkjet printing was carried out using a Dimatix DMP-2800 printer with 10 pl drop cartridges and a commercially-available silver-nanoparticle ink (DGP 40LT-15C by Anapro). After printing, the ink was cured in an oven for 60 min at 150 °C in air. Additional inkjet printing process details can be found in [5].

The nickel electro-deposition process was done in a nickel sulfamate bath at 54 °C under an electrical current density of 20 mA/cm^2.

Epoxy Chambers

The balloon actuator chambers were fabricated using 750-µm thick epoxy sheets (SUEX™ by DJ DevCorp) [6]. 5-mm diameter chambers and contact pad openings were patterned by photolithography and developed in PGMEA (Figure 1b). The usual post-exposure bake was replaced by the lamination step. The deep striations visible in the epoxy chambers disappeared after lamination. Thicker chambers were realized by stacking multiple sheets.

PDMS Membranes

The elastic membranes were made of PDMS (Sylgaard® 186 by Dow Corning) with a 10:1:5.5 mix ratio (base:catalyst:iso-octane). The elastomer was degassed under vacuum for 30 min and cast by pouring it on a 50-µm thick polyimide (PI) sheet (Kapton® E by Dupont) and leveled using a ZUA 2000 universal applicator (Zehntner GmbH).

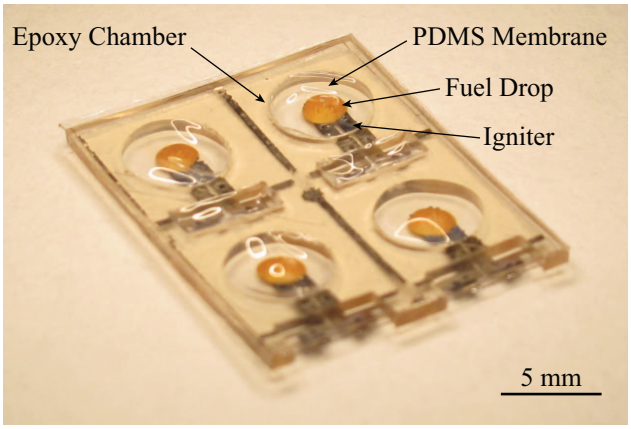

Figure 2: Photograph of a 2x2 matrix of pyroMEMS balloon actuators.

Lamination

Lamination of the different layers was carried out in a temperature-controlled press. Prior to lamination, silanization of the epoxy chambers was carried out using (3-Aminopropyl)triethoxysilane (APTES) to improve adhesion to the PDMS membrane. The PDMS membrane surface was activated with 15-second oxygen plasma treatment (400 sccm, 400 W) and the complete stack was immediately assembled. The stack was then placed into the press, loaded with 200 N (~5 bars) and heated for 90 min at 120 °C. A bonded, 2x2 matrix of pyroMEMS balloon actuators is shown in Figure 2. Stacks containing up to 3 epoxy layers were successfully bonded—taller stacks were not tested.

CHARACTERIZATION

Inkjet-printed Igniters

Both bare and nickel-plated inkjet-printed Ag igniters were tested to determine their maximum power before failure. For K-DNBF, roughly 1 W of input power for 1 s is required for ignition on a glass substrate [4]. The bare inkjet-printed igniters could not sustain these power levels—failing after 100 ms at 0.6 W—whereas the nickel-plated igniters performed nominally at 2.5 V (~1 W) for 1 s (Figure 3). By measuring the temperature coefficient of resistance of the igniters, the igniter temperature was inferred to be 265 °C—greater than the fuel's combustion temperature of 206 °C.

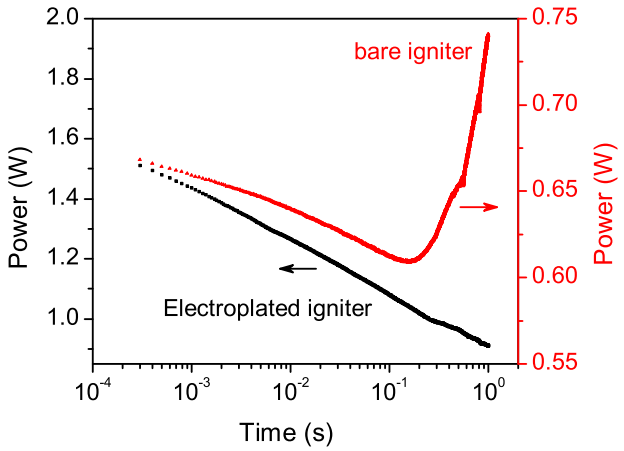

Figure 3: Igniter power dissipation (constant voltage). The 500 nm *Ni-plated igniter dissipated ~1* W *of power over 1* s*, while the bare igniter began failing after 100* ms *at 0.6* W*. (Note, y-scales are not the same).*

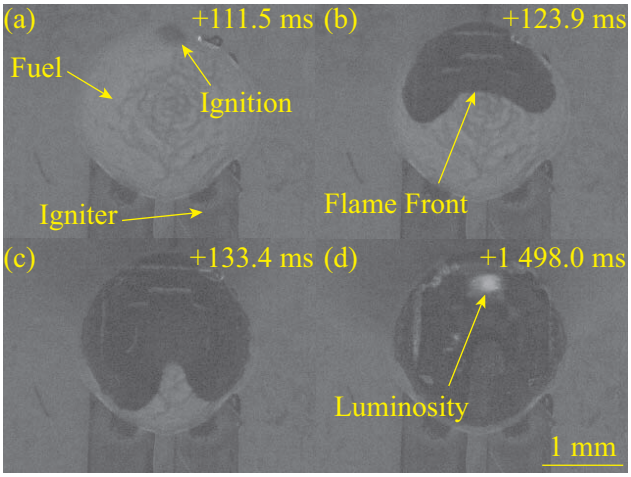

Figure 4: High-speed video frames of fuel combustion (20 % binder, ~1 W *input power): (a) ignition, (b)-(c) smooth flame spreading and (d) end of voltage pulse.*

Ignition of both the 10 % and 20 % binder mass fraction fuel drops was successfully achieved with the nickel-plated igniters. Figure 4 shows the ignition and smooth combustion of a 20 % binder fuel drop. Figure 4d clearly shows the igniter still operational and

incandescing after 1.5 s. In only 3 cases, the heat dissipated by the igniter/combustion punctured holes in the PET substrate and ruptured the igniter (Figure 5a); however, most of the time, both survived intact (Figure 5b). The igniter resistance before ignition was 5.77 ± 1.27 Ω and 6.03 ± 2.02 Ω afterwards. Polyethylene naphthalate (PEN) substrates with a higher glass transition temperature will be considered in the future. Polyimide (PI) was tested, but exhibited poor adhesion to the epoxy chambers.

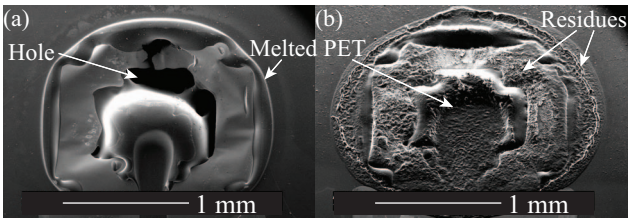

Figure 5: (a) SEM of a ruptured Ni-plated igniter (~1 W *for 1* s*). (b) SEM of an intact igniter after fuel combustion (same power/duration). Combustion residues are visible.*

PDMS Membranes

The PDMS membrane thickness (90±10 µm) was measured on its PI handling foil using a white-light interferometer (Veeco Wyko NT1100).

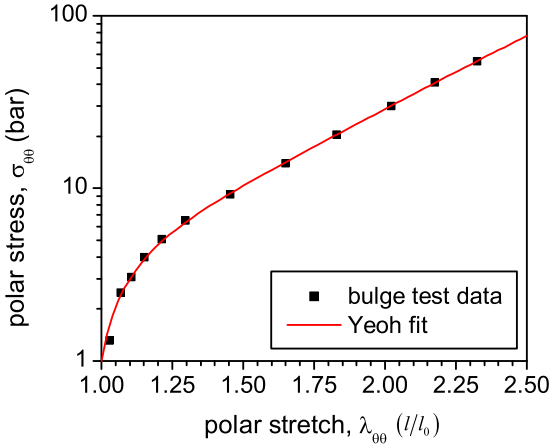

Figure 6: Polar stress/stretch data for the PDMS membranes fitted to a Yeoh biaxial hyperelastic model.

The mechanical response of the PDMS membranes to equibiaxial strain was characterized using a custom-built bulge-test setup. The PDMS membranes were bonded to a circular silicon holder by applying a 15-second oxygen plasma treatment (400 sccm, 400 W), immediately placed in contact with the Si holder. The holder was mounted on a manifold connected to a pressure controller (Druck DPI510). The membrane deflection was captured using a digital camera (Canon PowerShot G10). The membrane polar stretch, $\lambda_{\theta\theta}$—which is the ratio between the final and initial membrane arc lengths—was obtained by fitting circular arcs to the photographs using a custom MATLAB image recognition program. The thickness-averaged polar stress, $\sigma_{\theta\theta}$, as given in [7] is

$$\sigma_{\theta\theta} = \frac{\Delta P R_C \lambda_{\theta\theta}}{2e_0}, \qquad (1)$$

where ΔP is the pressure difference across the membrane, R_C is the balloon radius near the pole, e_0 is the unstretched membrane thickness. The polar stress/stretch data was then successfully fitted with a Yeoh equibiaxial hyperelastic model (Figure 6).

MODELING

A complete semi-analytical model of the pyroMEMS balloon actuator was developed. It divided the balloon inflation into two different steps: fuel combustion and membrane inflation. The following assumptions were used throughout: (1) ideal gas behavior, (2) adiabatic, impermeable walls, and (3) spherical cap membrane deflection.

First, a chemical kinetics program [8] was used to calculate the initial pressure, P_i, and the ratio of specific heats, γ, of the combustion products.

Second, the equilibrium membrane displacement is determined by equating the equilibrium pressure/volume below the membrane to the pressure needed to deform the membrane by that amount.

BALLOON TESTS

Experimental setup

A 1.5-second, 2.5 V square voltage pulse was applied to the igniters using a function generator (HP33120A) coupled to a high-speed power amplifier (NF Electronic Instruments 4015). Simultaneously, a high-speed framing camera (Vision Research Phantom v210) mounted onto a stereomicroscope acquired images of the combustion process at up to 21,000 frames per second.

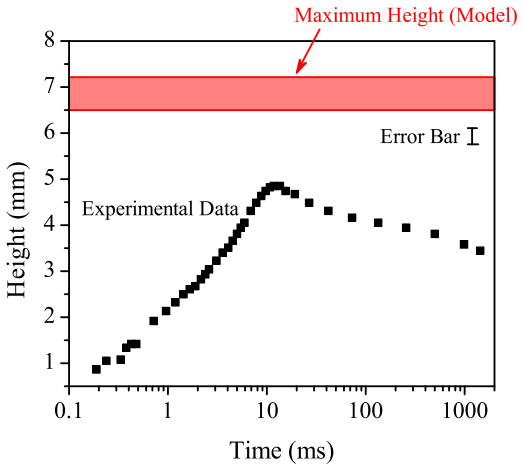

Figure 7: Balloon actuator height as a function of time (20 % binder, ~1 W *input power).*

Results

The pyroMEMS balloon actuators were successfully inflated (e.g., Figure 7 and 8). The balloon inflated to a maximum height of 5.8 ± 0.3 mm. The uncertainty in the model values was due to the uncertainty in the fuel mass.

Next, a series of pyroMEMS balloon actuators were inflated with different chamber volumes—from 1 to 3 epoxy layers thick. The maximum balloon heights were extracted from the high-speed videos and compared with

the semi-analytical model (Figure 9). The discrepancy between the experimental data and the semi-analytical model was between 28 % and 35 %.

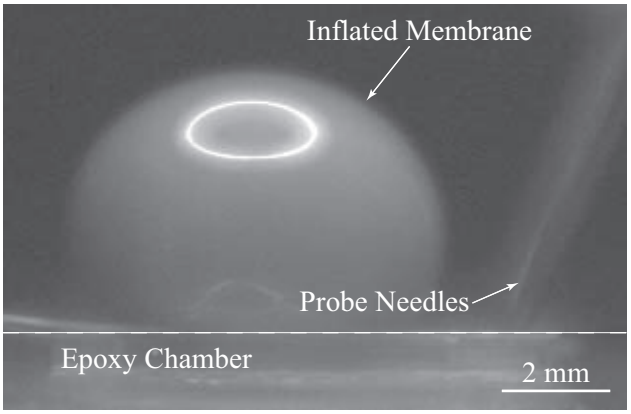

Figure 8: High-speed video frame of a pyroMEMS balloon actuator at maximum displacement (same as Figure 7).

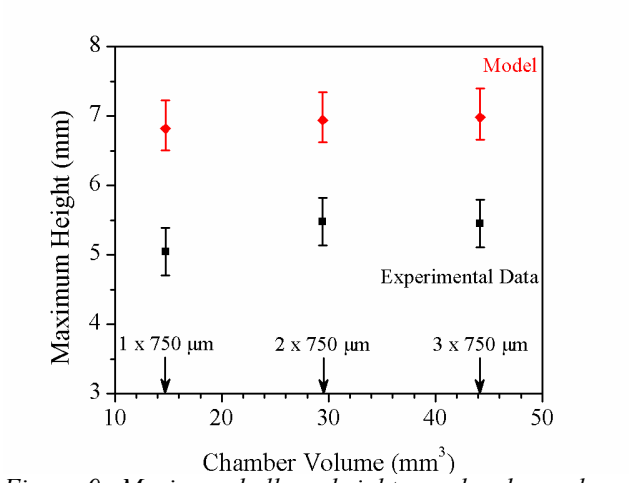

Figure 9: Maximum balloon height vs. chamber volume (20 % binder, ~1 W input power).

DISCUSSION

At first glance, the values generated by this simple model represent an overestimate on the maximum balloon height, due to unaccounted for heat losses and gas leakage. This is confirmed by the rapid deflation of the balloons—roughly 1/3 of their total height in one second. Parylene-C is known to be an effective sealing agent for PDMS [9]. This will be addressed in the future by evaporating a thin coating (~100 nm) of parylene-C on top of the PDMS membranes after lamination.

Furthermore, the ICT code was designed for and validated using macroscale solid propellant charges (i.e., 100 g): it remains an open question whether such models are applicable to the small fuel drops used in pyroMEMS devices. For example, in Figure 4 and in [4], K-DNBF—a primary explosive that detonates under normal conditions—undergoes slower, less energetic deflagration for fuel drops on the order of a few hundred micrograms. This is due to excessive thermal losses to the substrate.

CONCLUSIONS

PyroMEMS balloon actuators were successfully fabricated and tested using a low-cost, foil-level fabrication technique. The fabrication process was greatly simplified thanks to the maskless igniter fabrication and the thick epoxy sheets which is readily structured by photolithography and readily bonds to a number polymer substrates, such as PET and PDMS. The fabrication was easy and low-cost compared with standard microfabrication, which require Si-DRIE processing [2,3] and chip-level assembly [3].

ACKNOWLEDGEMENTS

The authors wish to thank Sara Talaei for help with foil lamination and Dr. Ulrich Bley at RUAG Ammotec GmbH for the K-DNBF. D. A. de Koninck gratefully acknowledges the financial support from the EPFL Space Center ESRP under contract #2007/033 as well as a postgraduate scholarship from the Natural Sciences and Engineering Research Council of Canada (NSERC).

REFERENCES

[1] C. Rossi, D. Estève, C. Mingués, "Pyrotechnic actuator: a new generation of Si integrated actuator", *Sens. Actuators A, Phys.*, vol. 74, pp. 211-215, 1999.

[2] G. A. A. Rodríguez, S. Suhard, C. Rossi, *et al.*, "A microactuator based on the decomposition of an energetic material for disposable lab-on-chip applications: fabrication and test", *J. Micromech. Microeng.*, vol. 19, 015006 (8pp.), 2009.

[3] D. Briand, P. Dubois, L.-E. Bonjour, *et al.*, "Large deformation balloon micro-actuator based on pyrotechnics on chip", in *Proc. IEEE MEMS 2008*, Tucson, January 13-17, 2008, pp. 535-538.

[4] D. A. de Koninck, D. Briand, L. Guillot, *et al.*, "Ignition and Combustion Behaviour in Solid Propellant Microsystems Using Joule-Effect Igniters", *J. Microelectromech. Syst.*, in press, doi: 10.1109/JMEMS.2011.2167667.

[5] F. Molina-Lopez, D. Briand, N. F. de Rooij, "All additive inkjet printed humidity sensors on plastic substrate", submitted to *Sens. Actuators B, Chem.*

[6] D. Johnson, A. Voigt, G. Ahrens, W. Dai, "Thick Epoxy Resist Sheets for MEMS Manufactuing and Packaging", in *Proc. IEEE MEMS 2010*, Hong Kong, January 24-28, 2010, pp. 412-415.

[7] N. Reuge, F. M. Schmidt, Y. Le Maoult, *et al.*, "Elastomer Biaxial Characterization Using Bubble Inflation Technique. I: Experimental Investigations", *Polym. Eng. Sci.*, vol. 41, pp. 522-531, 2001.

[8] Fraunhofer-Institut für Chemische Technologie, "ICT-Thermodynamic Code", [online] Available at: http://www.ict.fraunhofer.de/EN/coreco/EM/Ex/ICTcode/ICT-Code.jsp.

[9] S. Sawano, K. Naka, A. Werber, H. Zappe, S. Konishi, "Sealing method of PDMS as elastic material for MEMS", in *Proc. IEEE MEMS 2008*, Tucson, January 13-17, 2008, pp. 419-422.

CONTACT

*D. A. de Koninck, tel: +41.32.720.5442; david.dekoninck@epfl.ch